KATHOLIEKE UNIVERSITEIT
LEUVEN

Simultaneous Reconstruction of the Activity Image and Registration of the CT image in TOF-PET

Ahmadreza Rezaei, Johan Nuyts

Activity Reconstruction & Attenuation Registration

– *Attenuation Correction, Background*

- In clinical PET/CT,
  - The CT image is adjusted to the photon energy of 511 KeV.
  - The projections of the “adjusted CT” is then used for attenuation correction.
  - This “adjusted CT” is believed to be close enough to the true attenuation affecting the PET emission data.
    - Between-scan motion and in-scan motion can violate this assumption.
- The emission data can be corrected for attenuation:
  - When the emission data is affected by an affine transform of a known attenuation image.
    - F Natterer, 1993
    - A Welch, *et. al.*, 1998, A Bromiley 2001
    - A Alessio, *et. al.*, 2006
  - Time-of-flight data are available
    - A Rezaei, 2011, 2012
    - M Defrise, 2012, 2013
    - Y Nuyts, 2012

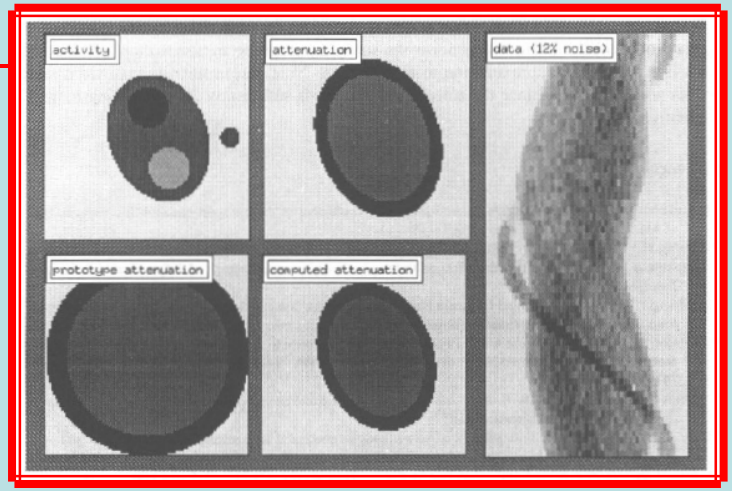

Joint Activity and Attenuation Reconstruction

– *MLAA*

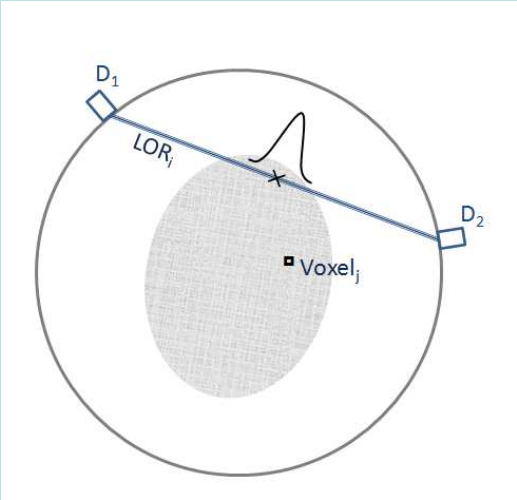

Sensitivity of (TOF-bin t and LOR i) to voxel j

Un-attenuated TOF Emission Sinogram

Emission Image

Additive Contributions (Scatter and/or Randoms)

$$p_{it} = \sum_j c_{ijt}\lambda_j$$

Expected counts

$$\bar{y}_{it} = a_i p_{it} + s_{it}$$

Attenuation Factors

$$a_i = e^{-\sum_j l_{ij}\mu_j}$$

Attenuation Image

Intersection of (LOR i) and voxel j

Poisson Log-likelihood for emission tomography:

$$L([\lambda,\mu],y) = \sum_{it} y_{it} \ln \bar{y}_{it} - \bar{y}_{it}$$

$$[\hat{\lambda}_{mle},\hat{\mu}_{mle}] = \underset{\lambda,\mu}{\operatorname{argmax}}\, L([\lambda,\mu],y)$$

TOF-MLEM

$$1:\ \mu^n, \lambda^{n+1} = \underset{\lambda}{\operatorname{arginc}}\, L([\lambda,\mu^n],y)$$

$$2:\ \lambda^{n+1}, \mu^{n+1} = \underset{\mu}{\operatorname{arginc}}\, L([\lambda^n,\mu],y)$$

MLTR

Activity Reconstruction & Attenuation Registration

– *Incorporating "side-information"*

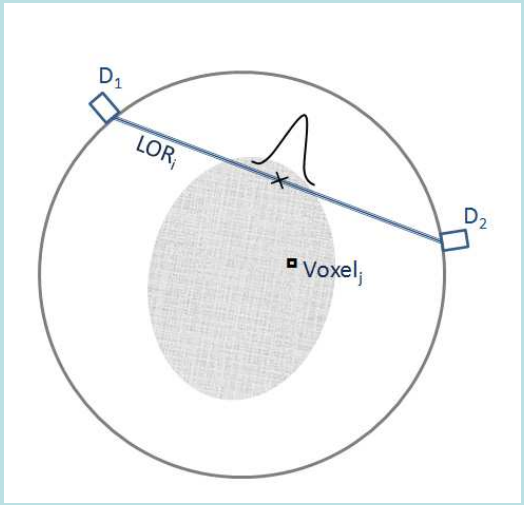

Un-attenuated TOF Emission Sinogram

Sensitivity of (TOF-bin t and LOR i) to voxel j

Emission Image

$$p_{it} = \sum_j c_{ijt}\lambda_j$$

Attenuation Factors

$$a_i = e^{-\sum_j l_{ij}\boldsymbol{D}\mu_j^0}$$

Deformed CT-converted Image

Intersection of (LOR i) and voxel j

Additive Contributions (Scatter and/or Randoms)

Expected counts

$$\bar{y}_{it} = a_i p_{it} + s_{it}$$

Poisson Log-likelihood for emission tomography:

$$L([\lambda, \boldsymbol{D}], y) = \sum_{it} y_{it} \ln \bar{y}_{it} - \bar{y}_{it}$$

$$[\hat{\lambda}_{mle}, \hat{\boldsymbol{D}}_{mle}] = \underset{\lambda,\boldsymbol{D}}{\operatorname{argmax}}\, L([\lambda, \boldsymbol{D}], y)$$

TOF-MLEM

$$1: \boldsymbol{D^n}, \lambda^{n+1} = \underset{\lambda}{\operatorname{arginc}}\, L([\lambda, \boldsymbol{D}^n], y)$$

$$2: \lambda^{n+1}, \boldsymbol{D}^{n+1} = \underset{\boldsymbol{D}}{\operatorname{arginc}}\, L([\lambda^{n+1}, \boldsymbol{D}], y)$$

MLTR-Demons'

Activity Reconstruction & Attenuation Registration

– *MLRR*

- MLRR Algorithm:

TOF-MLEM

$$\lambda_j^n = \frac{\lambda_j^{n-1}}{\sum_{it} c_{ijt} a_i^{n-1}} \sum_{it} c_{ijt} a_i^{n-1} \frac{y_{it}}{\bar{y}_{it}}$$

Update of MLTR

$$\Delta\mu = \frac{\sum_i l_{ij}(\bar{y}_i - y_i)}{\sum_i l_{ij} y_i \sum_k l_{ik}}$$

$$\boldsymbol{D}^n = \boldsymbol{D}^{n-1} + k \frac{(\Delta\mu)\boldsymbol{\nabla}\mu}{(\boldsymbol{\nabla}\mu)^2 + \alpha(\Delta\mu)^2}$$

Demons' Registration

- Non-rigid
- Optical flow
- Regularized

*

$$\mu_j^n = \boldsymbol{D}^n \mu_j^0$$

CT deformation

Moving Image *Fixed Image*

Optical Flow Equation: $-(M - F) = \boldsymbol{D}.\boldsymbol{\nabla}F$

Projection on $\boldsymbol{\nabla}F$

$$\boldsymbol{D} = \frac{-(M-F)\boldsymbol{\nabla}F}{\|\boldsymbol{\nabla}F\|^2}$$

To stabilize **D**

$$\boldsymbol{D} = \frac{-(M-F)\boldsymbol{\nabla}F}{\|\boldsymbol{\nabla}F\|^2 + \alpha(M-F)^2}$$

2D Simulations

– *Phantom & Demons' Registration Method*

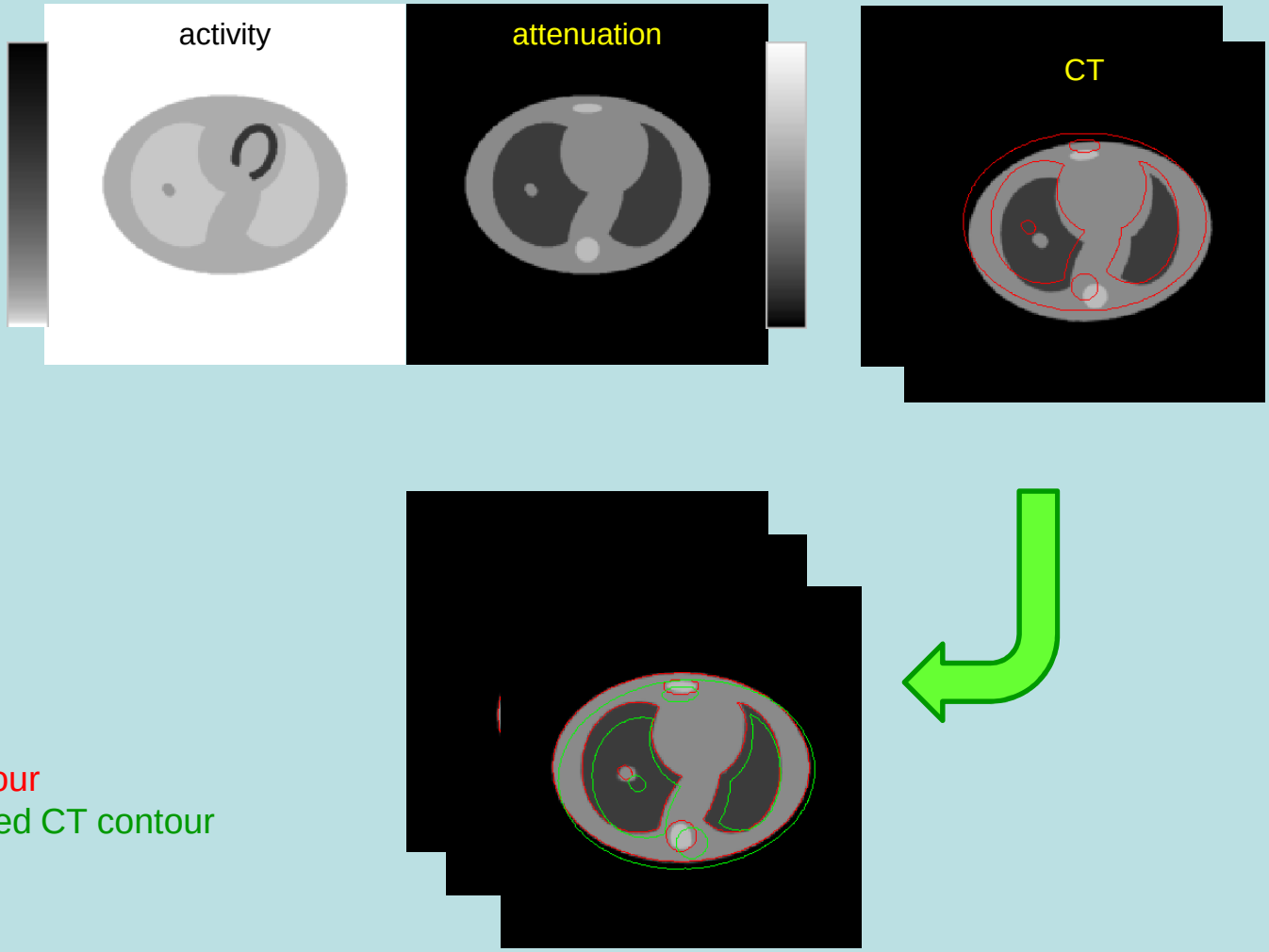

2D Simulations

– *Noiseless data*

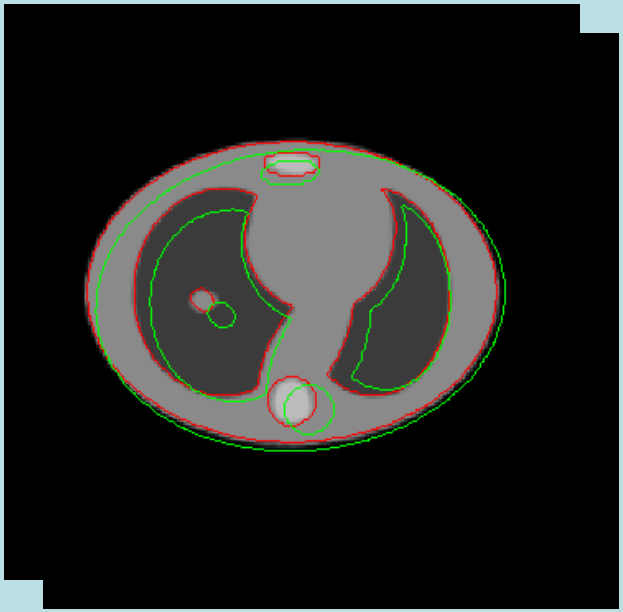

- Simulation specifications:
  - 200*200 thorax phantom
  - 168 projection angles over 180º
  - TOF resolution of 580ps
  - 13 TOF-bins of 312ps
  - Oversampling of 3 causing slight mismatch

** (#iterations : #subsets)

True contour

Mismatched CT contour

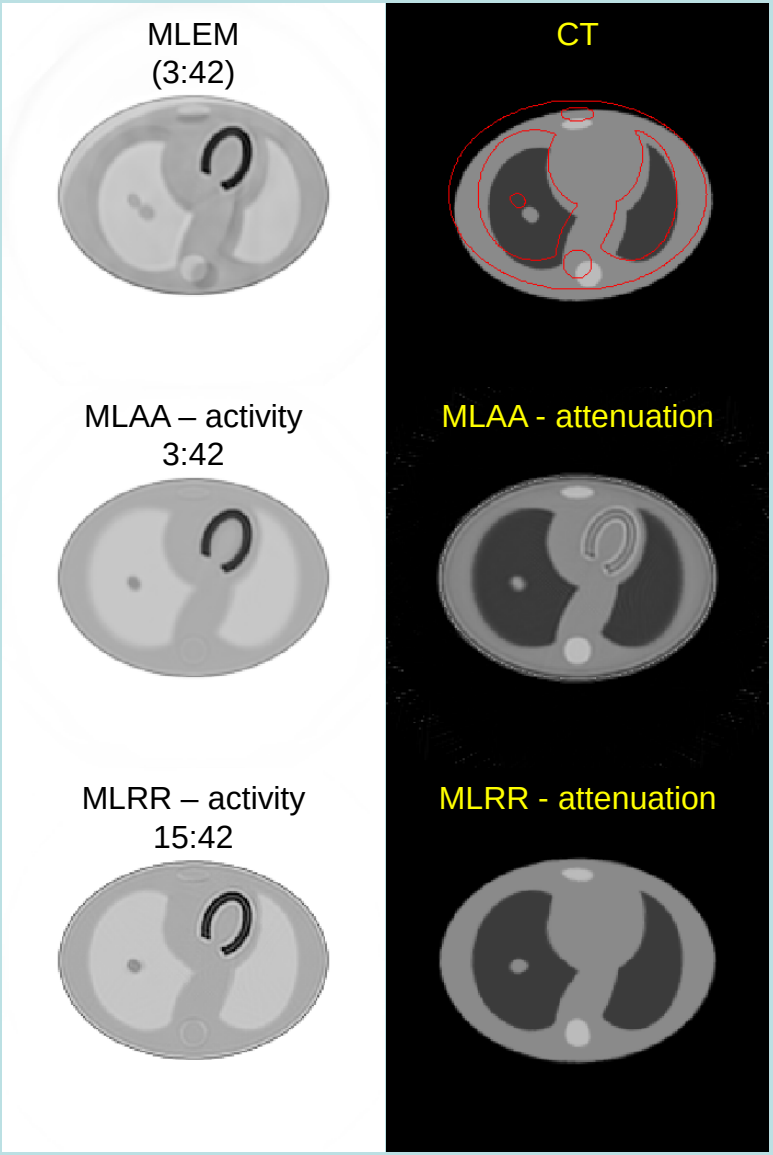

2D Simulations

– *Noisy data*

MLEM
(3:42)

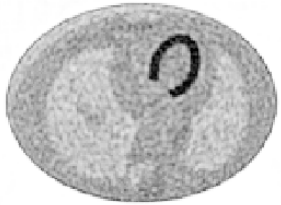

MLAA activity
(3:42)

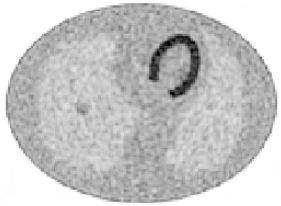

MLRR activity
(15:42)

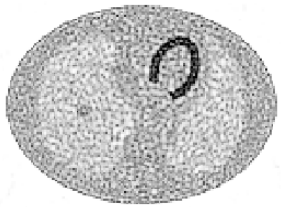

MLAA attenuation

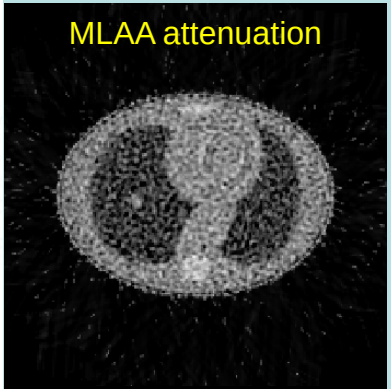

MLRR attenuation

MLEM
(3:42)

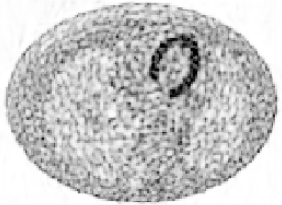

MLAA activity
(3:42)

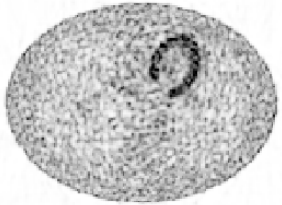

MLRR activity
(15:42)

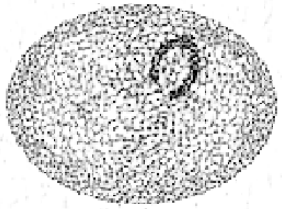

MLAA attenuation

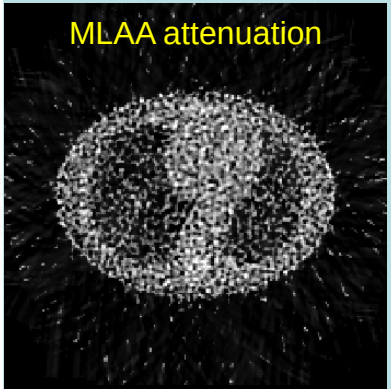

MLRR attenuation

2D Simulations

– *Noisy data*

MLEM
(3:42)

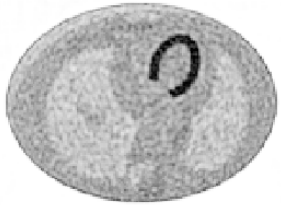

MLAA activity
(3:42)

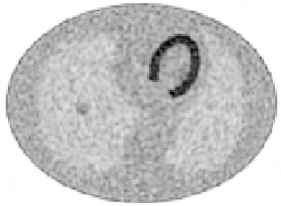

MLRR activity
(15:42)

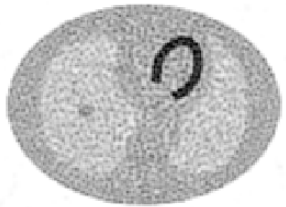

FWHM=0.6cm

MLAA attenuation

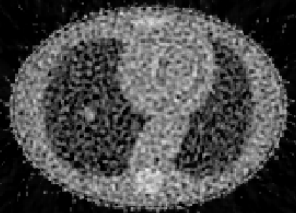

MLRR attenuation

MLEM
(3:42)

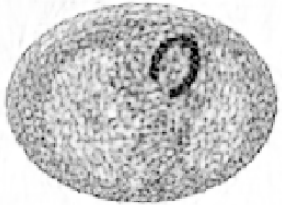

MLAA activity
(3:42)

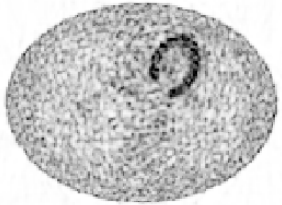

MLRR activity
(15:42)

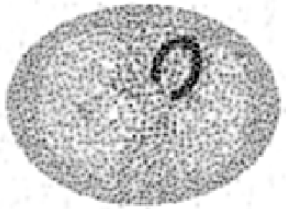

FWHM=0.6cm

MLAA attenuation

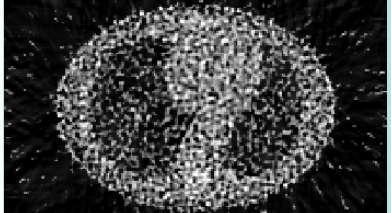

MLRR attenuation

2D Simulations

– *Looking at displacements*

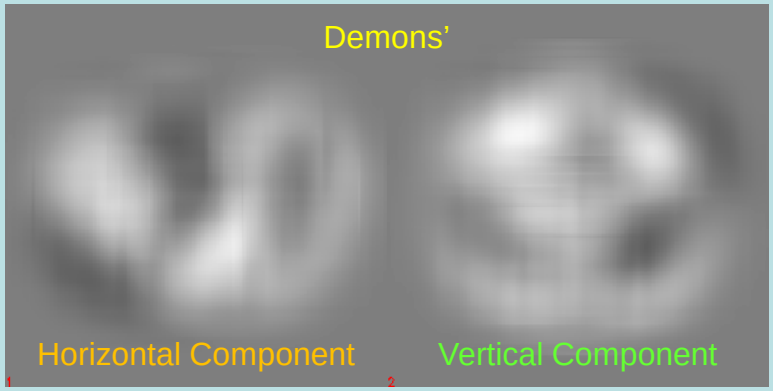

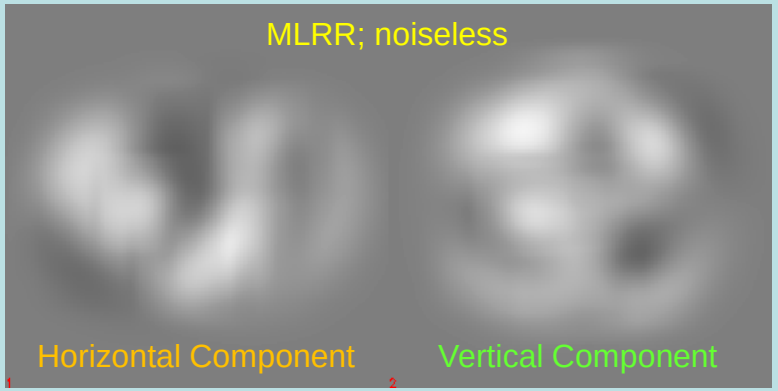

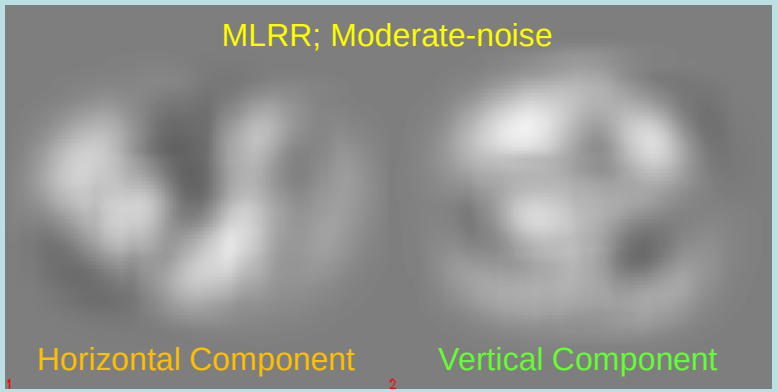

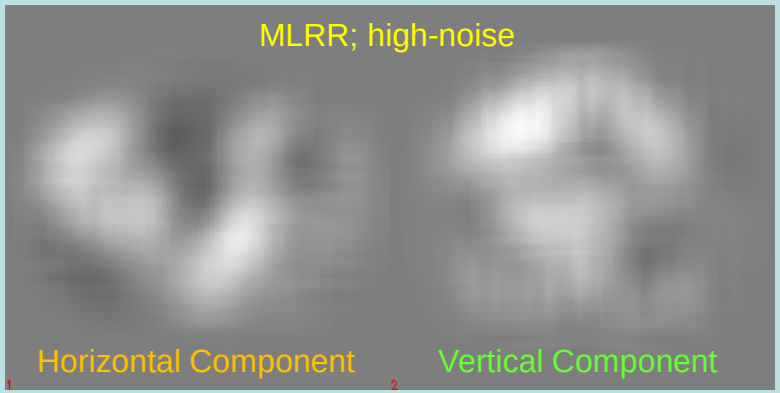

3D Simulations

– *XCAT Phantom*

- XCAT Phantom
  - # of frames: 8
  - Maximum Diaphragm motion: 2.0 cm
  - Max AP Expansion: 1.2 cm
  - Respiratory Motion: True
  - Heart Motion: False

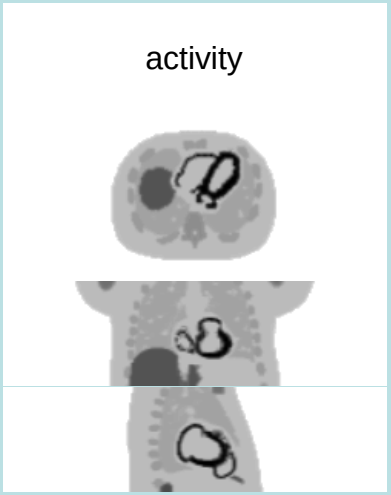

- Simulation specifications:
  - 200*200*109 phantom
  - 7 oblique segments
  - Span 1*
  - 168 projection angles over 180º
  - TOF resolution of 580ps
  - 13 TOF-bins of 312ps

** (#iterations : #subsets)

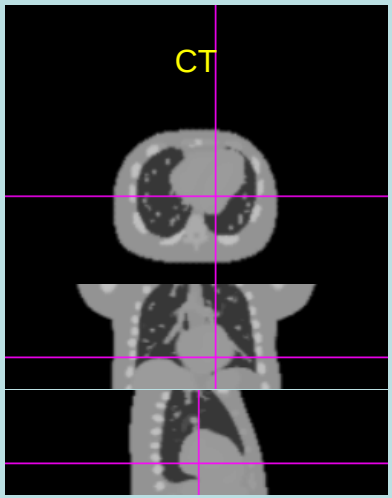

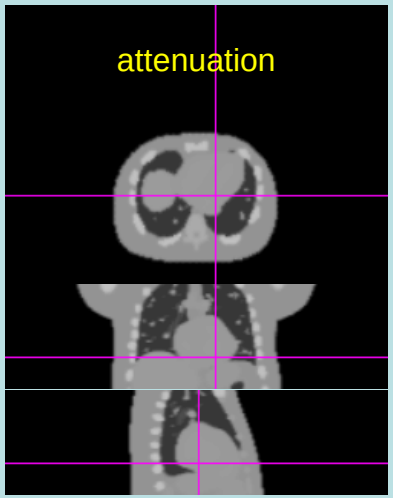

3D Simulations

– *MLEM, MLAA & MLRR*

MLEM
(3:42)

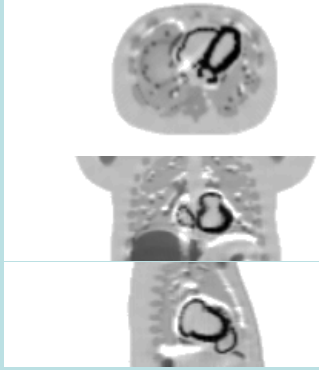

TOF-MLEM
(3:42)

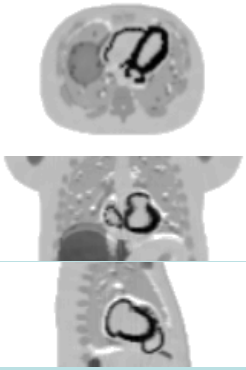

MLAA activity
(3:42)

MLRR activity
10:42

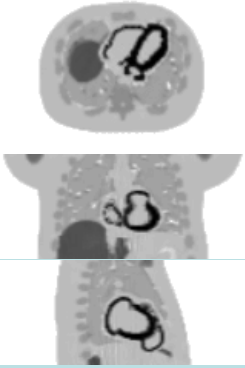

CT

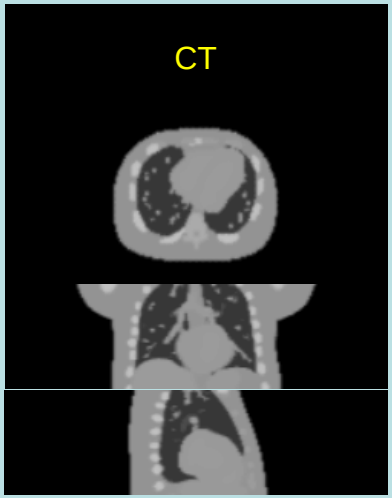

MLAA attenuation

MLRR attenuation

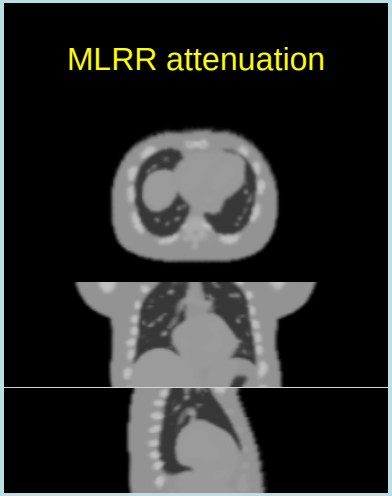

3D Simulations

– *Residual Errors*

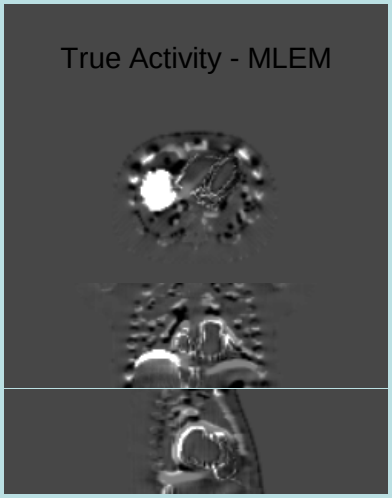

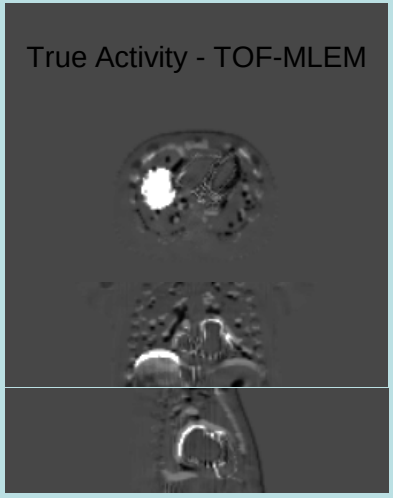

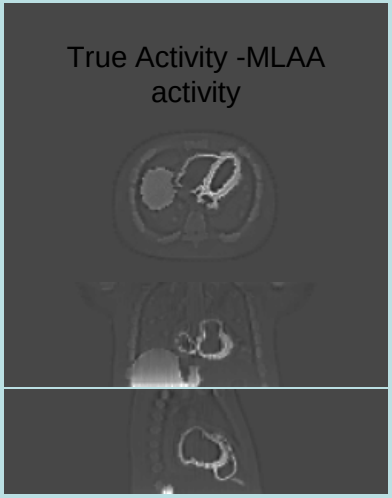

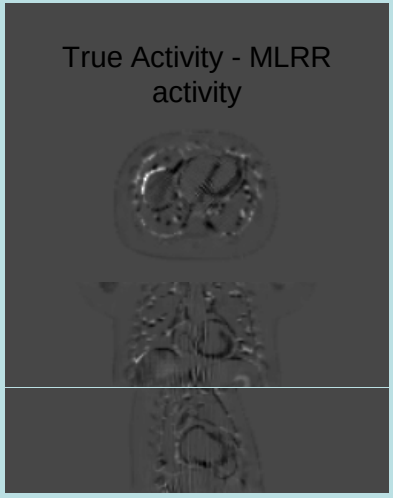

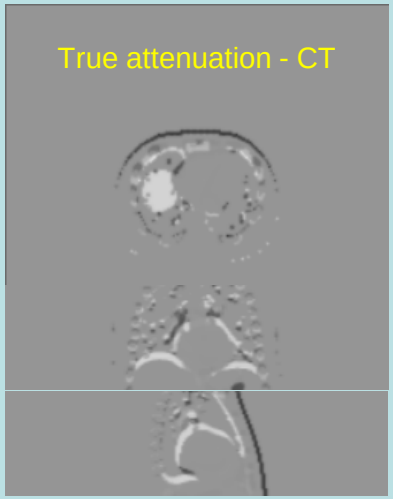

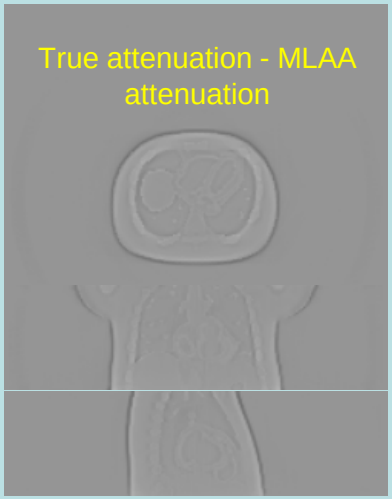

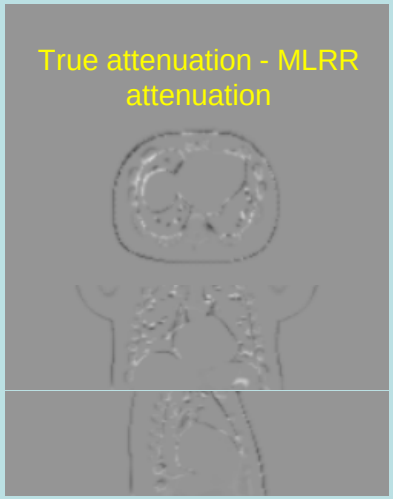

3D Simulations

– *Absolute Residual Errors*

Absolute
True Activity - MLEM

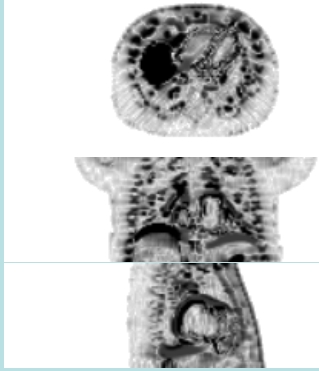

Absolute
True Activity - TOF-MLEM

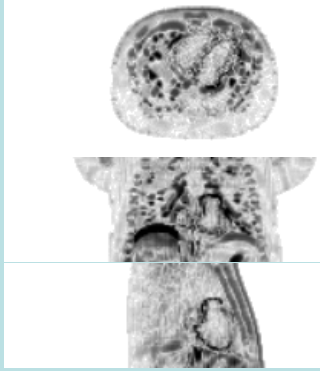

Absolute
True Activity -MLAA activity

Absolute
True Activity - MLRR activity

Absolute
True attenuation - CT

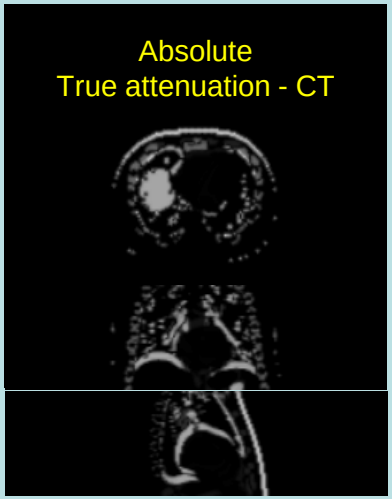

Absolute
True attenuation - MLAA attenuation

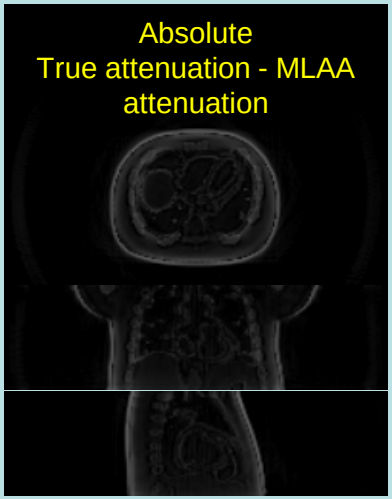

Absolute
True attenuation - MLRR attenuation

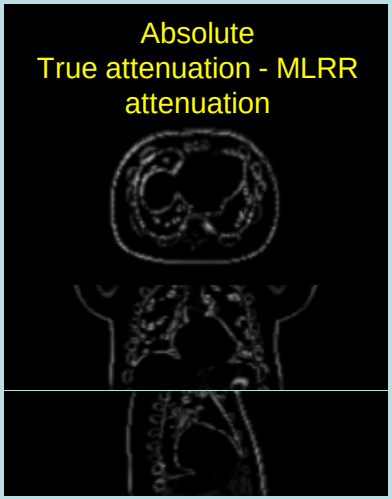

Patient Data

– *MLEM, MLAA & MLRR*

MLEM
(3:42)

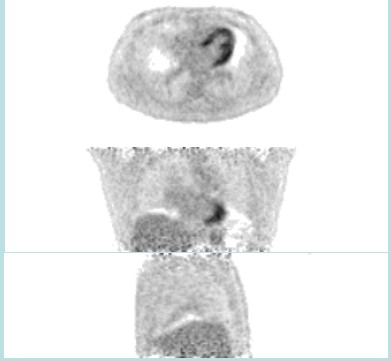

TOF-MLEM
(3:42)

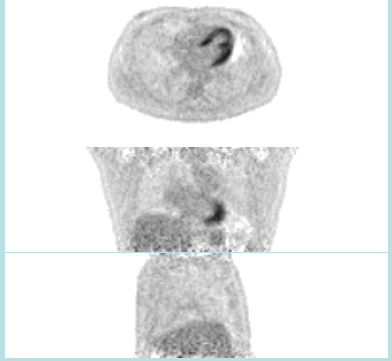

MLAA activity
(3:42)

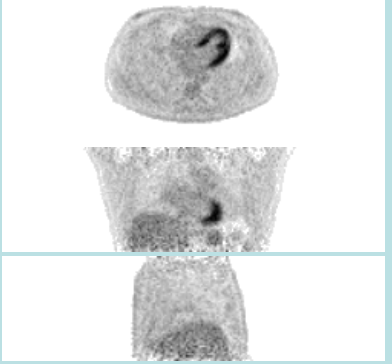

MLRR activity
(5:42)

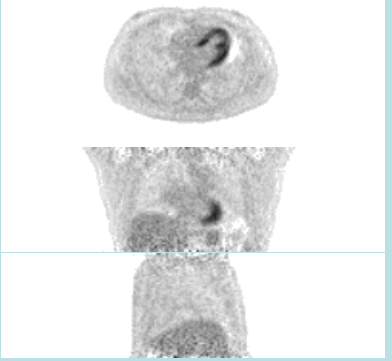

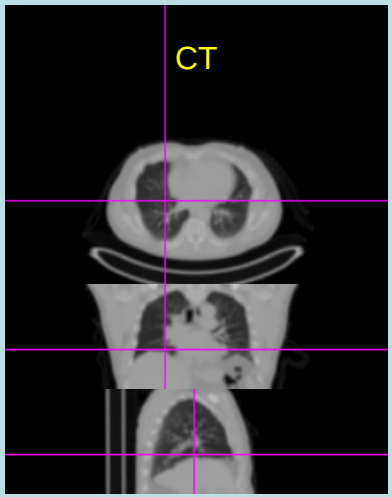

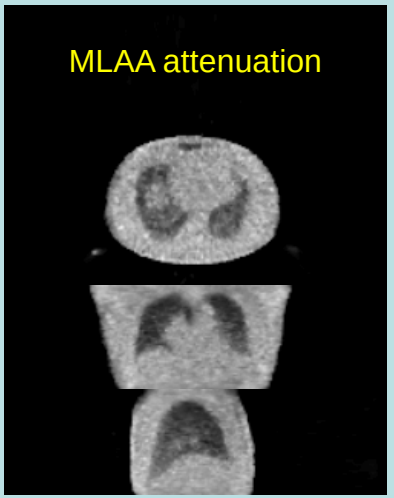

Patient Data

– *MLEM; Gated data from listmode*

- Amplitude-based Gating
  - W van Elmpt 2011, Optimal gating compared to 3D and 4D PET reconstruction, *Eur J Nucl Med Mol Imaging,* 38:843-855.

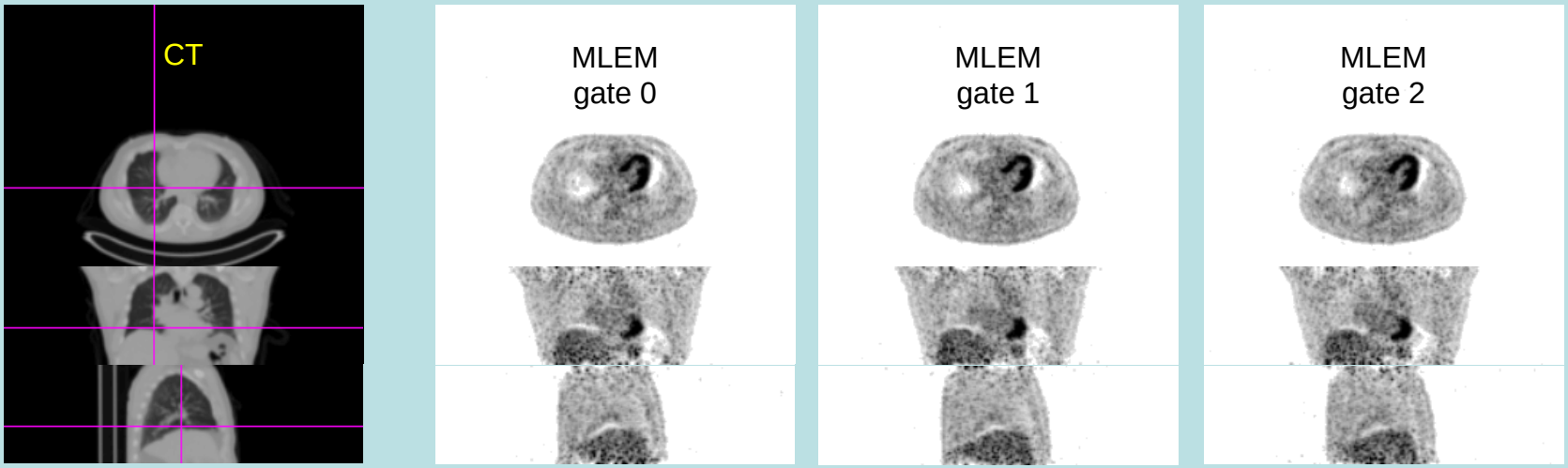

Patient Data

– *MLEM; Gated data from listmode*

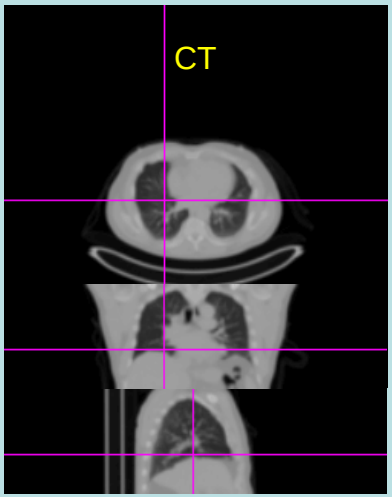

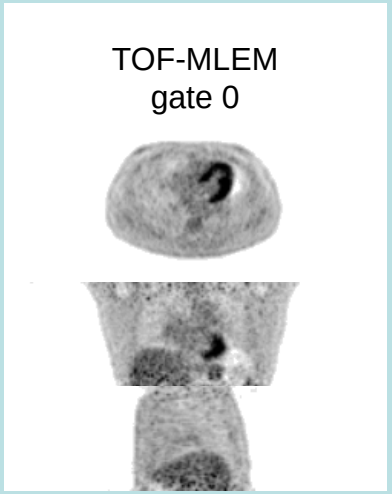

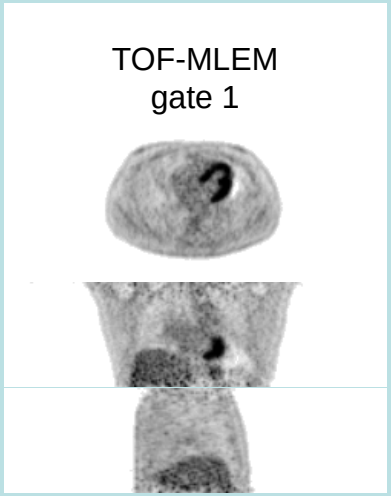

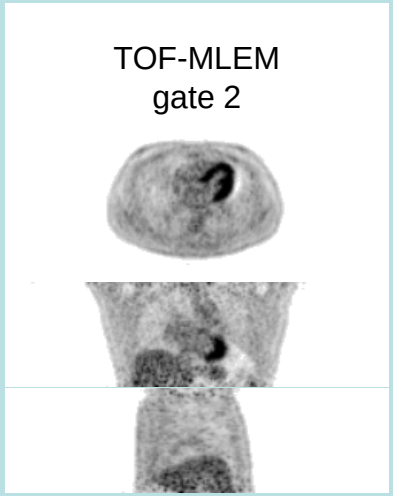

Patient Data

– *MLAA; Gated data from listmode*

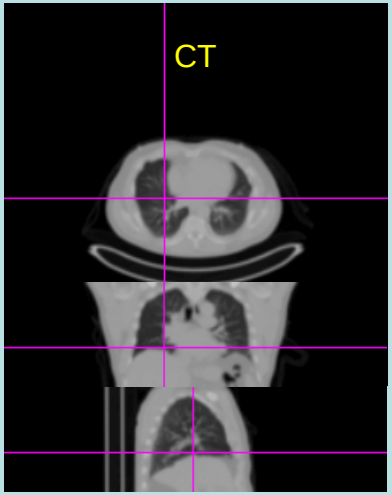

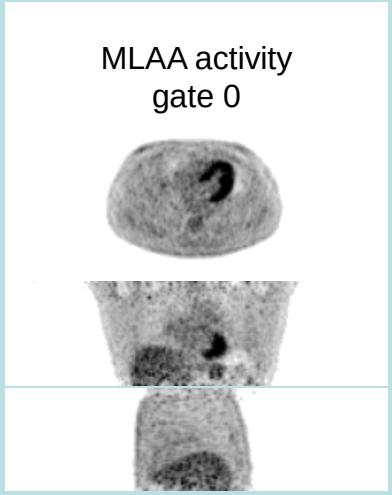

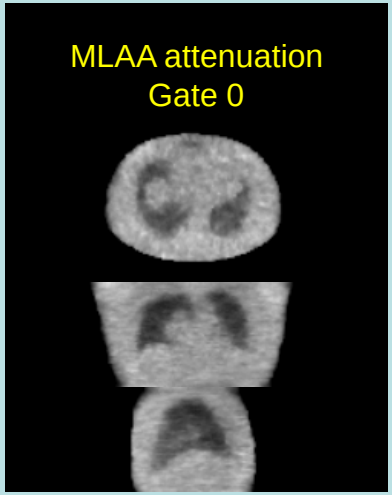

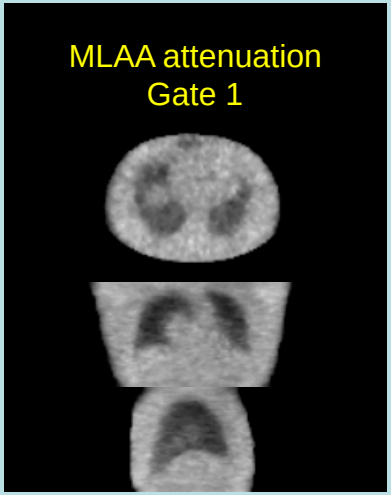

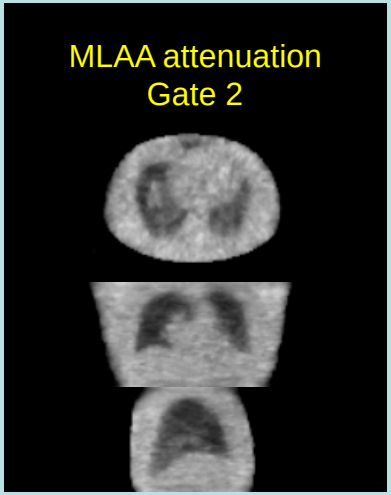

Patient Data

– *MLRR; Gated data from listmode*

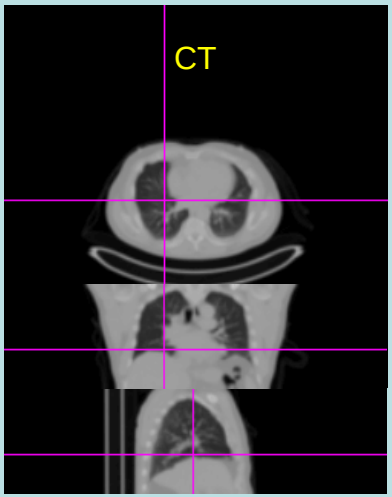

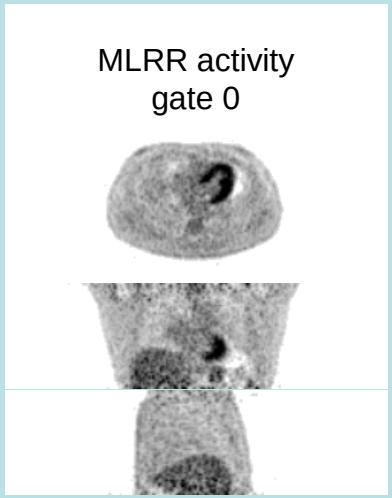

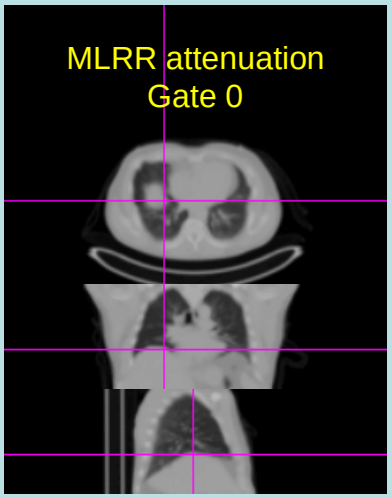

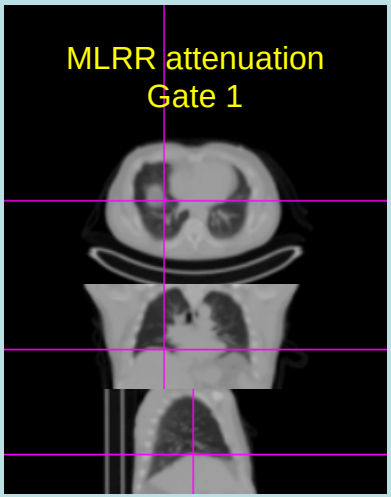

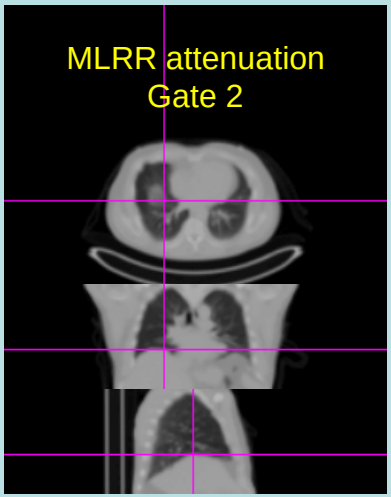

Patient Data

– *Difference Images*

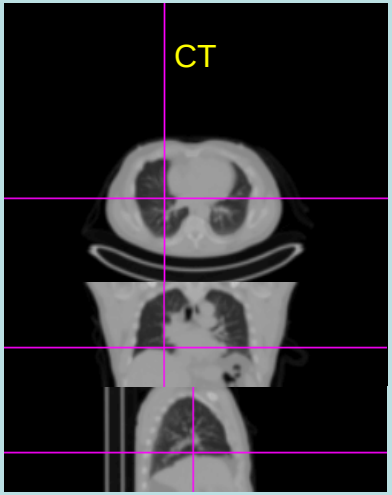

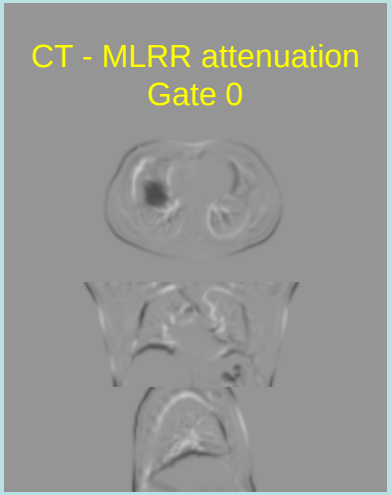

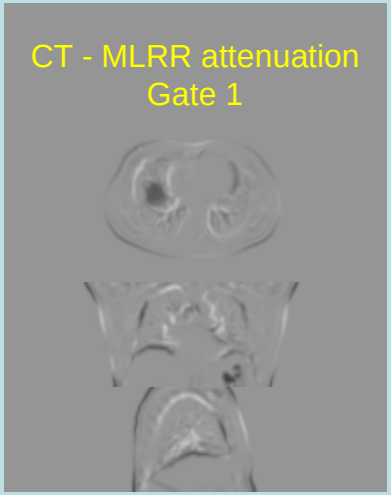

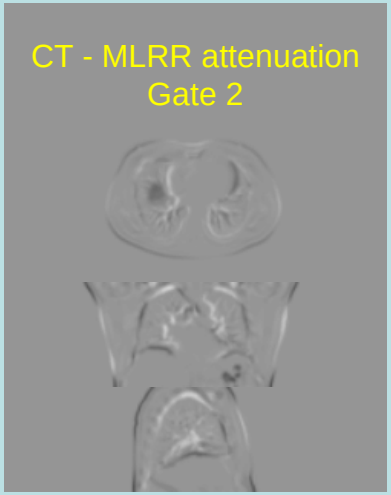

Conclusions & Future Work

- MLRR is proposed to make use of high quality CT scans.
- Our 2D/3D simulations indicate:
  - MLRR is able to produce aligned activity and attenuation reconstructions similar to MLAA, with two advantages:
    - The scale problem is solved!
    - High quality, noise-free attenuation reconstructions are made available.
- The clinical results show:
  - Good agreement of MLRR attenuation reconstructions and expected breathing patterns.
  - More accurate activity reconstructions near boundaries affected by motion (compared to MLEM activity reconstructions with the CT-derived attenuation).
- Future Work:
  - Incorporate physical properties of different tissue types.
  - Because the emission data from a moving attenuation is inconsistent, analyzing the gated reconstructions seems to be the only way to quantitative reconstruction in the presence of motion.

- Our thanks to:
  - **Michel Defrise** from the Vrije Universiteit Brussel, and **Annemie Ribbens** from KU Leuven for the very insightful discussions.
  - **Mike Casey**, **Judson Jones** from Siemens Healthcare, Molecular Imaging for the data-based gating software and data processing.
  - **S Stroobants**, **S Staelens** and **M Lambrechts** from the Universiteit Antwerpen for the patient data.
  - **You!** for your attention. ☺